Molecular Mechanism of Inhibition of Nonclassical FGF-1 Export[†,‡]

Dakshinamurthy Rajalingam,[§] Thallapuranam Krishnaswamy S. Kumar,[§] Raffaella Soldi,[||] Irene Graziani,[||] Igor Prudovsky,[||] and Chin Yu*[,§,⊥]

Department of Chemistry and Biochemistry, University of Arkansas, Fayetteville, Arkansas 72701, Center for Molecular Medicine, Maine Medical Center Research Institute, Scarborough, Maine 04074, and Department of Chemistry, National Tsing Hua University, Hsinchu 30043, Taiwan

Received August 11, 2005; Revised Manuscript Received September 27, 2005

ABSTRACT: Fibroblast growth factor (FGF-1) lacks a signal sequence and is exported by an unconventional release mechanism. The nonclassical export of FGF-1 has been shown to be inhibited by an anti-allergic and anti-inflammatory drug, amlexanox (AMX). We investigate the molecular mechanism(s) underlying the inhibitory action of AMX on the release of FGF-1, using a variety of biophysical techniques including multidimensional NMR spectroscopy. AMX binds to FGF-1 and enhances its conformational stability. AMX binds to locations close to Cys30 and sterically blocks Cu^{2+}-induced oxidation, leading to the formation of the homodimer of FGF-1. AMX-induced inhibition of the formation of the FGF-1 homodimer is observed both under cell-free conditions and in living cells. Results of this study suggest a novel approach for the design of drugs against FGF-1-mediated disorders.

Proteins released through the conventional secretory pathway mediated by the endoplasmic reticulum (ER)[1] and the Golgi apparatus contain a signal peptide sequence at the amino-terminal end (*1*). However, there are several extracellular proteins, such as interleukin 1α (IL1α), IL1*β*, fibroblast growth factors 1 and 2, transglutaminase, sphingosine kinase 1, annexin 2, and the proteins belonging to the S100 family, that lack the signal peptide sequence but are secreted into the extracellular medium (for a review, see refs *2* and *3*). Although the mechanism(s) of release of proteins through the nonclassical pathways is not fully understood, it is now a subject of intensive investigation.

Prototype fibroblast growth factor 1 (FGF-1) is a signal peptide-less, heparin-binding protein, devoid of intramolecular disulfide bonds (*4*, *5*). FGF-1 regulates a wide array of important biological processes such as angiogenesis, differentiation, tumor growth, and neurogenesis (*4*). Although FGF-1 acts through specific transmembrane tyrosine kinase receptors, it lacks a classical signal peptide to direct its secretion to the extracellular compartment (*6*). Under normal conditions, FGF-1 is not released from cells that express it. FGF-1 is shown to be secreted from FGF-1-transfected cells in response to stress conditions *in vitro*, such as hypoxia and heat shock (*2*). Stress-induced release of FGF-1 from the FGF-1-transfected NIH 3T3 cells occurs through a brefeldin A-insensitive, ER−Golgi-independent pathway. It is believed that the nonclassical release of FGF-1 is an inherent protective mechanism developed during the course of evolution to regulate the high mitogenic potential and widespread expression of FGF-1 (*2*). In this context, it is interesting to note that recombinant FGF-1 expressed with an N-terminal signal sequence behaves as a potent oncoprotein (*8*).

Under stress conditions, FGF-1 is released as an inactive homodimer that is unable to bind to heparin (*7*). The mitogenic activity of FGF-1 may be completely regained in the presence of reducing agents, such as dithiothreitol, suggesting that the homodimer is formed because of an intermolecular disulfide bond (*2*, *7*, *9*). Site-directed mutagenesis studies revealed that the FGF-1 homodimer released into the extracellular medium is formed because of selective oxidation of the thiol group of highly conserved Cys30 (*10*; Figure 1A). Results of cell-free experiments showed that the formation of the FGF-1 homodimer is due to the Cu^{2+}-induced oxidation of the thiol group of Cys30 (*11*). It is noteworthy that treatment with tetrathiomolybdate (TTM), a specific copper chelator, was demonstrated to suppress FGF-1 release in cell culture (*12*), and it dramatically inhibits the accumulation of FGF-1 and intimal hyperplasia (restenosis) in the walls of rat carotid arteries in response to balloon angioplasty (*15*). However, additional experiments are required to unequivocally prove that formation of the homodimer is a mandatory mechanism for the stress-induced release of FGF-1 into the extracellular compartment.

It was demonstrated that the anti-allergic and anti-inflammatory drug, amlexanox (AMX, Figure 1B), which inhibits the degranulation of mast cells, is also able to inhibit the release of FGF-1 (*13*, *14*). *In vitro* studies revealed that

[†] This study was supported by grants from the National Institutes of Health (NIH NCRR COBRE Grant 1 P20 RR15569) and National Science Council, Taiwan, to C.Y. and from the Arkansas Biosciences Institute to C.Y. and T.K.S. This work was supported in part by NIH Grants HL32348, HL35627, and RR15555 to I.P.

[‡] The article is dedicated to the memory of Tom Maciag, scientist and friend.

* To whom all correspondence should be addressed. E-mail: cyu@uark.edu. Fax: 479-575-4049. Telephone: 479-575-5646.

[§] University of Arkansas.

[||] Maine Medical Center Research Institute.

[⊥] National Tsing Hua University.

[1] Abbreviations: FGF, fibroblast growth factor; ER, endoplasmic reticulum; AMX, amlexanox; IL1α, interleukin 1α; IL1*β*, interleukin 1*β*; TTM, tetrathiomolybdate; HSQC, heteronuclear single-quantum coherence.

10.1021/bi0516071 CCC: $30.25
Published on Web 11/04/2005

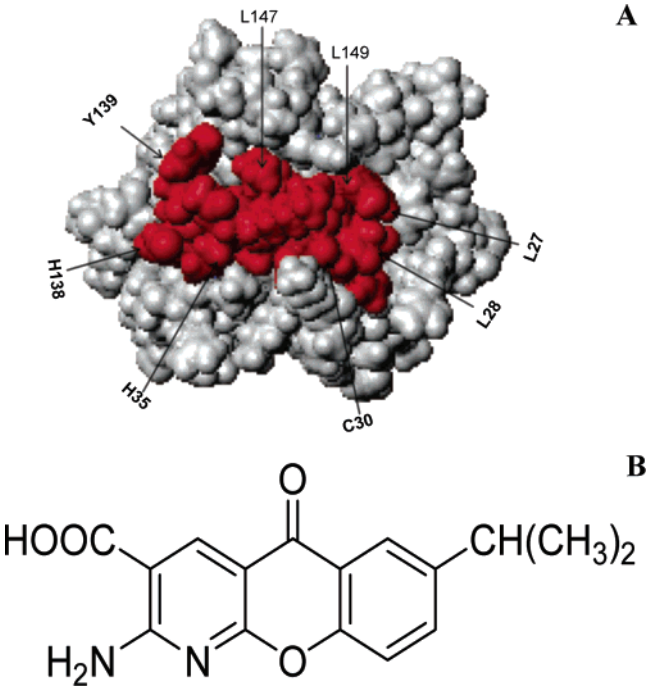

FIGURE 1: (A) MolMol representation of the three-dimensional structure of FGF-1. The residues involved in AMX binding are shown in red. (B) Chemical structure of AMX.

cells exposed to AMX exhibit a dose-dependent inhibition of migration and proliferation without an increase in apoptotic cell death (*14*). AMX affects the organization of actin stress fibers without attenuating the expression and polymerization of actin (*14*). The inhibitory effect of AMX on FGF-1 release is believed to be at least partially linked to the effect(s) of the drug (AMX) on the actin cytoskeleton (*14*). In the present study, we demonstrate that AMX directly binds to human FGF-1 and blocks Cu^{2+}-induced homodimerization of the protein. These results emphasize the importance of dimerization of FGF-1 for its stress-induced release into the extracellular compartment.

MATERIALS AND METHODS

Ingredients for Luria Broth were obtained from AMRESCO. Aprotinin, pepstatin, leupeptin, phenylmethylsulfonyl fluoride, TritonX-100, 1-anilino-8-naphthalene sulfonate (ammonium salt), and β-mercaptoethanol were obtained from Sigma. Heparin-Sepharose was obtained from Amersham Biosciences. Labeled $^{15}NH_4Cl$ and D_2O were purchased from Cambridge Isotope Laboratories. The other chemicals used were of high-quality analytical grade. The experiments were performed at 25 °C. Unless specified, solutions were made in 10 mM tris buffer (pH 7.5) containing 100 mM NaCl. AMX was obtained from Takeda Company, Japan.

Protein Purification. Overexpression and purification of human FGF-1 was achieved using methods reported by Arunkumar et al. (*16*). ^1H, ^{15}N, and ^{13}C resonance assignments and the three-dimensional structure of FGF-1 were reported by Ogura et al. (*17*).

Turbidity Measurements. Turbidity measurements were performed on a Hitachi U-3310 spectrophotometer. All measurements were made after 30 s of incubation of FGF-1 with 0.1 mM $CuCl_2$ and 0.2 mM AMX at room temperature. The concentration of the protein used in the turbidity experiments was 100 μM. The turbidity of the solutions was measured by absorbance at 600 nm. The path length of the sample cell used was 10 mm.

Steady-State Fluorescence. Fluorescence experiments were performed on a Hitachi F2500 spectrofluorimeter at 5 or 10 nm resolution. Intrinsic fluorescence measurements were made at a protein concentration of 50 μM, using an excitation wavelength of 280 nm. For the thermal denaturation experiments, the protein and AMX were mixed in a 1:1 ratio in 10 mM tris buffer (pH 7.5) containing 100 mM NaCl. The requisite temperature(s) in the thermal denaturation experiments was attained using a NesLab circulating water bath.

Proteolytic Digestion Assay. The limited proteolytic experiments on FGF-1 and the FGF-1−AMX mixture (1:1) were carried out (at 25 ± 2 °C) using trypsin. Proteolytic digestions were performed at an enzyme (trypsin)/substrate (FGF-1) molar ratio of 1:100. The protease activity was stopped after a desired time interval by the addition of the gel loading dye (Bio-Rad) at 80 ± 2 °C. The degree of proteolytic cleavage was measured from the intensity of the ~16-kDa band (on a SDS−PAGE gel) corresponding to the uncleaved protein (FGF-1), using a densitometer. The intensity of the ~16-kDa band (corresponding to FGF-1) not subjected to protease treatment was considered as a control for 100% protection against trypsin cleavage.

Isothermal Calorimetry. Binding of AMX to FGF-1 was analyzed by measuring the heat change during the titration of AMX into the protein solution using VP-ITC titration microcalorimeter (MicroCal, Inc., Northampton, MA). All protein and ligand (AMX) solutions were degassed under vacuum and equilibrated at 25 °C prior to titration. The sample cell (1.4 mL) contained 0.2 mM FGF-1 dissolved in 10 mM tris buffer (pH 7.5) containing 100 mM NaCl. The reference cell contained water. Upon equilibration, 2 mM AMX drug was injected in 47 × 6 μL aliquots using the default injection rate of 200 s intervals between each injection to allow the sample to return to the baseline. The resulting titration curves were corrected for the protein-free buffer control and analyzed using the software supplied by Microcal, Inc.

NMR Experiments. All NMR experiments were performed on a Bruker Avance-700 MHz NMR spectrometer equipped with a cryoprobe at 25 °C. ^{15}N decoupling during acquisition was accomplished using the globally optimized altering-phase rectangular pulse sequence. Spectra were acquired with 8 transients of 1024 data points and 64 t_1 increments. The HSQC spectra were recorded at 32 scans at all concentrations of AMX. The concentration of the protein sample was 0.5 mM in 95% H_2O and 5% D_2O [10 mM tris (pH 7.5)] containing 100 mM NaCl. All of the spectra were processed on a Windows workstation using Xwin-NMR and Sparky softwares (*18*).

Molecular Docking. Molecular docking of FGF-1 and AMX was performed using the *ab initio* docking software BiGGER (*19*). The docking procedure is composed of two modules that work in a sequence. The first module (BoGIE, boolean geometric interaction evaluation) is a grid-like search algorithm, which generates a population of docked geometries with maximal surface matching and favorable intermolecular amino acid contacts. The first step is the generation of a three-dimensional matrix composed of small cubic cells of 1 Å size, which represents the complex shape of each

molecule. For every relative orientation of two interacting molecules, the translational interaction space is searched by systematically shifting the matrixes defining one molecule (the probe, AMX) relative to the matrixes representing the other partner (the target, FGF-1). Structures involving unrealistic interpenetration of the docking partners are discarded. The second module (INTERACT) evaluates the population of putative solutions according to four different interaction terms (surface matching, side-chain contacts, electrostatic, and solvation energies) combined into a global scoring function and computed for every docked geometry. The structures of the FGF-1/AMX complex as obtained by the docking algorithm filtered by NMR data (^{1}H-^{15}N chemical-shift perturbation data) were first minimized in a preparation step, using the conjugate-gradient method by the Powell algorithm. All parameters were minimized. Then, a molecular dynamics calculation (AMBER force field) was performed on the selected complex structures. The final energy minimized structure of the FGF-1/AMX complex was represented using the MolMol software (*20*).

Measurement of Amide Proton Exchange. Protein solutions with or without AMX (at a 1:1 protein/drug ratio) were prepared in 10 mM tris buffer (pH 7.5) containing 100 mM NaCl and dried by lyophilization (*21*, *22*). Hydrogen−deuterium (H/D) exchange is initiated by dissolving dry protein in 10 mM tris-buffered D_2O (pD 7.5, at 25 °C). All NMR data acquisition parameters were preset using a mock sample, and the sample pH was measured after the experiment, to minimize the dead time. The first ^{1}H-^{15}N HSQC spectrum was acquired within 10 min of initiation of exchange. Spectra were acquired with 8 transients of 1024 data points and 64 t_1 increments. A total of 50 spectra were collected in 48 h with various time points. Amide proton exchange was measured by monitoring the peak intensities in the ^{1}H-^{15}N HSQC spectra acquired after various time periods of exchange. The percentage proton occupancy values of residues in FGF-1 (in the presence or absence of AMX) were estimated from the intensities of individual ^{1}H-^{15}N cross-peaks in the ^{1}H-^{15}N HSQC spectra of the protein, acquired at different time points after initiation of the hydrogen−deuterium (H/D) exchange. The intensities of individual cross-peaks in the first ^{1}H-^{15}N HSQC spectrum (acquired within 10 min of initiation of H/D exchange) are considered equivalent to 100% proton occupancy. ^{1}H-^{15}N HSQC spectra were referenced internally to a nonexchangeable aliphatic proton resonance in the one-dimensional ^{1}H spectra.

Study of the AMX Effect in Living Cells. Stable FGF-1 NIH 3T3 cell transfectants were plated in DMEM (Cellgro) supplemented with 10% fetal calf serum (HyClone) on human fibronectin-coated (10 μg/cm^2) 15 cm dishes. To evaluate the effect of AMX upon the FGF-1 dimer formation, cells were preincubated for 12 h with 0.375 mM AMX (Takeda). After preincubation, AMX-treated cells were transferred to serum-free medium with 0.375 mM AMX and 10 units/mL heparin (Sigma) and incubated for an additional 2 h at 37 or 42 °C. Control cells were incubated under similar conditions without AMX. After temperature stress, cells were lysed in Laemmlie loading buffer without mercaptoethanol (nonreducing conditions) and 10% of cell lysate derived from each dish was resolved in 15% SDS−PAGE. To assess the effect of AMX on FGF-1 release, conditioned media were collected from heat-shocked and control dishes, filtered, and incubated for 2 h at 37 °C with 1.25 μg/mL dithiothreitol. FGF-1 was isolated from conditioned media by using heparin sepharose chromatography as previously described (*28*) and loaded to 15% SDS−PAGE. Resolved proteins were transferred to Hybond C (Amersham), immunoblotted using anti-FGF-1 polyclonal antibodies, and visualized using the ECL kit (Amersham).

RESULTS AND DISCUSSION

The molecular mechanism(s) underlying the AMX-induced inhibition of the nonclassical release of FGF-1 is not clearly understood. The inhibitory action of AMX on the nonclassical release of FGF-1 could be due to several factors. (i) FGF-1 is characterized to be a Cu^{2+}-binding protein (*12*). AMX can possibly bind near the Cu^{2+}-binding sites in the monomeric state of FGF-1. As a consequence, AMX can inhibit the formation of the FGF-1 homodimer by steric masking of the thiol group of Cys30 from oxidation induced by Cu^{2+}. The formation of the FGF-1 homodimer may be mandatory for its (FGF-1) release into the extracellular medium. (ii) There is a sequence of predicted molecular events that eventually leads to the release of FGF-1 into the extracellular medium (*2*). The predicted initial step is the interaction of the FGF-1 homdimer with S100A13, a calcium-binding protein belonging to the S100 family (*23*). FGF-1 is exported out into the extracellular compartment through a complex chain of molecular events that are not clearly understood (*2*). In principle, AMX can bind to any of the protein players (involved in the release pathway) and disrupt/interfere with the predicted chain of protein−protein interactions involved in the release of FGF-1. (iii) AMX may also alter the membrane properties and thereby inhibit the transmembrane translocation of the FGF-1. To understand the exact mode of action of AMX, we investigated the binding of the drug (AMX) using several physical methods including NMR spectroscopy.

AMX Binds to the Monomeric State of FGF-1. Isothermal titration calorimetry (ITC) is a direct method to evaluate the stoichiometry, affinity, and enthalpy of binding reactions in solution and has been successfully employed to characterize the binding of small ligands to their protein partners (*24*). In this context, we used ITC to examine whether FGF-1 has an affinity to bind to AMX. AMX binds to FGF-1; this interaction is endothermic (Figure 2). The equilibrium dissociation constant (K_d) defining the protein/drug interaction is about 80 μM, suggesting that the drug binds to the protein with moderate affinity. The FGF-1/AMX-binding isotherms are best represented as a one independent site model, yielding a stoichiometry of binding equal to 1 AMX molecule/molecule of FGF-1. The binding of FGF-1 proceeds with a positive enthalpy, suggesting that nonpolar interactions play a predominant role in the protein/drug interaction.

FGF-1 Is Stabilized by AMX Binding. FGF-1 contains a single well-conserved tryptophan at position 121 (*5*). The emission spectrum of the protein is dominated by a tyrosine emission peak at 308 nm. However, in the completely unfolded state (in 8 M urea), FGF-1 exhibits an emission spectrum dominated by tryptophan fluorescence at 350 nm. These spectral features are ideal to monitor the denaturant-induced unfolding of the protein. Equilibrium thermal

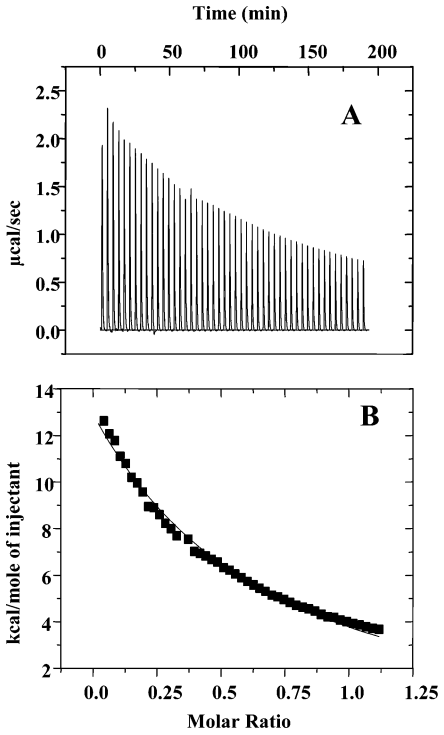

FIGURE 2: Isothermogram representing the binding of AMX to FGF-1 at 25 °C. (A) Raw data of the titration of the protein with AMX. (B) Integrated data obtained from the raw data, after subtracting the heat of dilution. The solid line (B) represents the best curve fit to the data, using the one independent site mode (from MicroCal Origin).

denaturation of FGF-1 was performed to assess the conformational stability of FGF-1 upon binding to AMX (Figure 3A). The T_m (the temperature at which 50% of the molecules are in the native state) of the protein increases in the presence of the drug by about 5 °C (from 55 to 60 °C), suggesting that thermodynamic stability of the protein is enhanced upon binding to the drug.

Limited proteolytic digestion is a popular technique to probe the protein−ligand interactions (*25*). Proteolytic digestion, in general, is governed not only by stereochemistry and accessibility of the protein substrate but also by the specificity of the proteolytic enzyme. In principle, binding of a ligand/drug can potentially mask the cleavage sites in the protein substrate, and these subtle differences in the cleavage patterns (between the free and the ligand/drug-bound protein substrate) could be easily detected by SDS−PAGE analysis. Because FGF-1 is rich in arginine and lysine residues, we opted to perform a limited trypsin digestion to probe the binding of AMX to FGF-1. Time-dependent trypsin digestion of the protein (in the free and AMX-bound forms) was monitored by SDS−PAGE analysis. The degree of digestion was measured on the basis of the intensity (after Coomassie Blue staining) of the ~16-kDa band (on the polyacrylamide gel) corresponding to the undigested FGF-1. SDS−PAGE analysis of the tryptic digests of FGF-1, obtained in the presence and absence of AMX, clearly revealed that the protein upon binding to the drug is more resistant to proteolytic cleavage (Figure 3B). The enhanced resistance to trypsin cleavage could be due to masking of some of the potential enzyme cleavage sites in FGF-1 by AMX. Interestingly, an additional low molecular cleavage product (M_r < 5 kDa) is observed when FGF-1 is subjected to limited

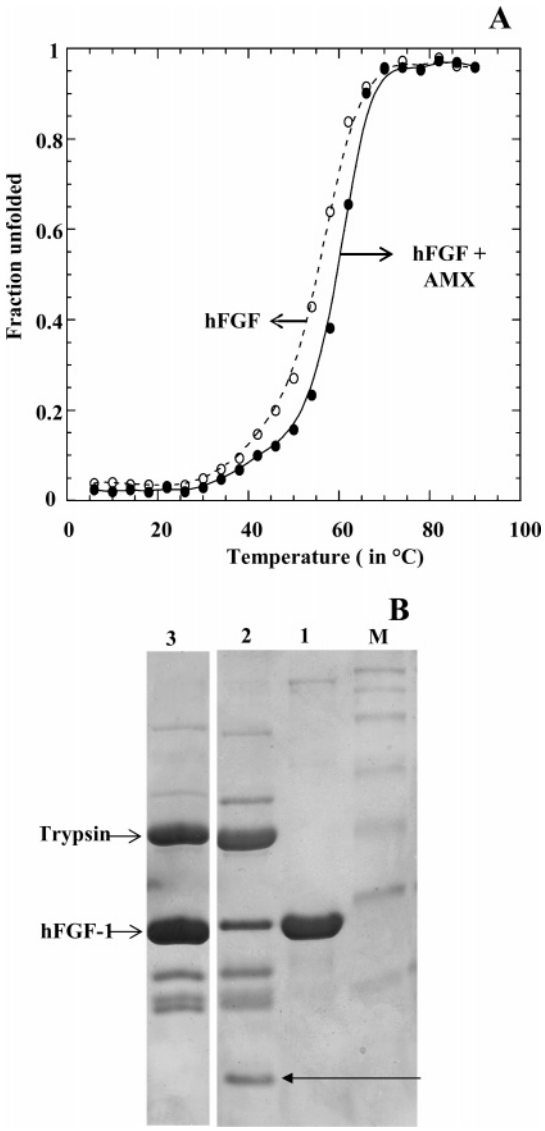

FIGURE 3: (A) Thermal denaturation of FGF-1 in the presence (●) and absence (○) of AMX. AMX binds to FGF-1 and stabilizes the protein by about 5 °C. (**B**) Limited trypsin digestion of FGF-1 monitored by SDS−PAGE. Lane M, protein marker; lane 1, untreated FGF-1; lane 2, FGF-1 treated with trypsin; lane 3, FGF-1 treated with trypsin in the presence of AMX. It could be observed that the protein in the presence of AMX is more resistant to trypsin cleavage. An extra cleavage product (indicated by an arrow) is generated when the protein is treated with trypsin in the absence of AMX. Control experiments revealed that the drug presence does not have inhibitory effects on trypsin.

trypsin digestion in the absence of AMX (lane 2 in Figure 3B). This extra cleavage product is not observed in the tryptic digest of FGF-1 obtained in the presence of AMX (lane 3 in Figure 3B). These results clearly indicate that AMX binds to FGF-1 and sterically restricts the exposure of the trypsin cleavage sites at the drug-binding site. In addition, size-exclusion chromatography experiments show that increased resistance of the protein to proteolytic cleavage is not due to protein oligomerization induced upon drug binding (Yu et al., unpublished data).

Cys30 Is a Part of the AMX-Binding Site in FGF-1. NMR spectroscopy is a versatile technique to map the protein−drug interface at an atomic resolution and also to measure the binding affinity and stoichiometry of protein−ligand interactions (*26*). The ^1H-^{15}N HSQC spectrum is a fingerprint

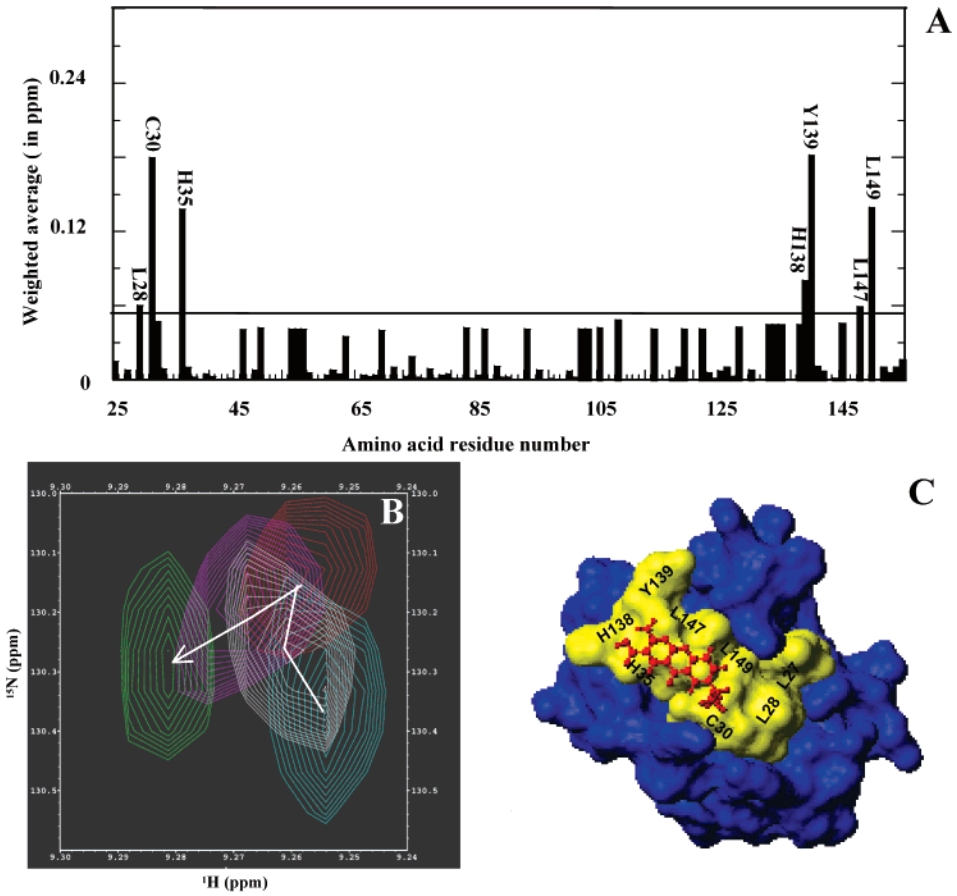

FIGURE 4: (A) Weighted average (of ^{15}N and ^{1}H) chemical-shift perturbation [$\Delta\delta = \sqrt{(\delta H^2 + 0.2(\delta^{15}N)^2)}$] of residues in FGF-1 upon complex formation with AMX (at a protein/AMX ratio of 1:1). It could be discerned that Leu28, Cys30, His35, His138, Tyr139, Leu147, and Leu149 displayed maximal chemical-shift perturbation. These residues constituted the putative AMX-binding site. The horizontal line is an arbitrary line drawn to demarcate residues, which exhibit significant chemical-shift perturbation from those that show insignificant chemical perturbation (<0.07 ppm). (B) Overlays of the Cys30 cross-peak in the ^{1}H-^{15}N HSQC spectra of FGF-1 obtained at increasing concentrations of AMX. Blue, white, red, pink, and green spectra correspond to protein/AMX ratios of 1:0, 1:0.2, 1:0.4, 1:0.6, and 1:1, respectively. The arrow indicates the direction of the shift of the cross-peak corresponding to Cys30 in the ^{1}H-^{15}N HSQC spectra. It can be seen that the cross-peak representing Cys30 shows a progressive chemical shift, suggesting its involvement in the binding of AMX. (C) MolMol representation of the structure of FGF-1 (blue) bound to AMX (red). The residues, which exhibit prominent chemical-shift perturbation, are indicated in yellow. The residues constituting the drug-binding site are mostly located in β-strands XII and I in the FGF-1 molecule.

of the conformational state(s) of the protein. Each cross-peak in the spectrum represents an amino acid in a particular conformational state of the protein. Therefore, the ligand-binding site(s) in a protein could be conveniently identified by a chemical-shift perturbation/disappearance of cross-peaks in the ^{1}H-^{15}N HSQC spectrum. ^{1}H-^{15}N HSQC spectra of FGF-1 acquired at various FGF-1/AMX ratios revealed that only a few cross-peaks were perturbed from their original positions in the native-state spectrum (Figure 4A and supplementary Figure S1 in the Supporting Information). The residues, which exhibit prominent ^{1}H-^{15}N chemical-shift perturbations, include Leu28, Cys30, His35, His138, Tyr139, Leu147, and Leu149 (parts A and B of Figure 4). In addition, the ^{1}H-^{15}N cross-peak corresponding to Leu27 disappeared (even at a AMX/protein ratio of 0.2:1.0) because of kinetic line-broadening effects. The residues in the AMX-binding pocket span β-strands I and XII constituting the β-barrel architecture of the FGF-1 molecule (*5*). Modeling the FGF-1 and AMX interface using BiGGER software based on the ^{1}H-^{15}N chemical-shift data indicated that the residues, which bind to the drug, were located in close proximity in the three-dimensional structure of FGF-1 (Figure 4C). Titration curves generated on the basis of the weighted average chemical-shift perturbation values of individual residues corroborated with the ITC data and demonstrated that the stoichiometry of binding of FGF-1/AMX is 1:1 (supplementary Figure S2 in the Supporting Information).

Amide−proton exchange monitored by NMR spectroscopy is a versatile technique to monitor conformational flexibility of proteins and to map protein−protein or protein−ligand interface(s) (*27*). In general, solvent accessibility to the transiently unfolded portions of proteins allows the exchange of the amide protons for deuterons to take place on time scales that range from hours to days (*27*). Amide protons involved in the protein−protein or protein−ligand interface are expected to be relatively more shielded from exchange. Therefore, the binding interface can be easily identified by comparing the exchange rates in the absence and presence of the interacting protein or ligand. We mapped the AMX-binding sites on FGF-1 by hydrogen−deuterium exchange monitored by ^{1}H-^{15}N HSQC spectra (Figure 5). A comparison of exchange rates of the amide protons in FGF-1, in the absence and presence of AMX, revealed that the amide protons of residues involved in the FGF-1/AMX interface (Leu27, Leu28, Cys30, His35, His138, Tyr139, Leu147, and Leu149) exhibited relatively higher protection to exchange

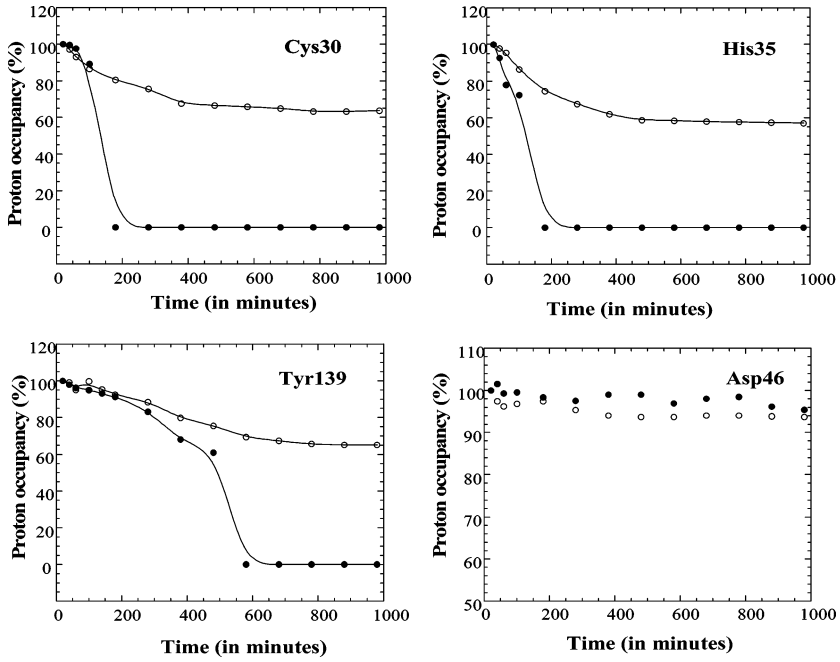

FIGURE 5: Amide proton exchange of selected residues in FGF-1 in the presence (○) and absence (●) of AMX. It could be observed that the residues involved in the AMX-binding site show significantly higher protection in the presence of the drug than in its absence. Asp46 is not involved in AMX binding, and hence, its amide proton exchange is representative for residues (in FGF-1) not involved in drug binding. The amide proton-exchange data clearly suggest that Cys30, His138, and Tyr139 are part of the AMX-binding site in the protein.

than those residues that are located at sites remote from the drug-binding sites (Figure 5). Interestingly, in the presence of AMX, the amide proton occupancy of Cys30 was more than 80%, suggesting that the drug bound to FGF-1 and protected the amide proton of Cys30 from hydrogen−deuterium exchange.

AMX Prevents the Cu^{2+}-Induced Oxidation of Cys30. As mentioned earlier, the homodimer of FGF-1 released under stress conditions is formed because of the specific oxidation of the thiol group of Cys30 (*10*, *11*). Interestingly, Cys30 is located in the putative AMX-binding site. In this background, we examined whether binding of AMX could prevent the formation of the Cu^{2+}-induced homodimer of FGF-1 *in vitro*. SDS−PAGE analysis demonstrated that, in the absence of AMX, Cu^{2+} induced formation of the FGF-1 homodimer (lane 3 in Figure 6B). In contrast, under similar experimental conditions, AMX thwarts the formation of the Cu^{2+}-induced homodimer of FGF-1 (lane 2 in Figure 6B). The homodimer of FGF-1 induced by Cu^{2+} undergoes time-dependent aggregation. Therefore, we studied the effect(s) of AMX on the Cu^{2+}-induced homodimerization of FGF-1 by turbidometric measurements at 600 nm. In the absence of AMX, the 600 nm absorbance progressively increases and reaches a steady plateau within 200 s of the addition of copper (Figure 6A). It is noteworthy, in the presence of AMX (at a protein/AMX ratio of 1:1), that there is no significant increase in the 600 nm absorbance even after 5 h of the addition of copper. Collectively, the results of turbidometry and SDS−PAGE analysis unambiguously suggest that AMX inhibits the formation of the Cu^{2+}-induced homodimer in a cell-free system.

AMX Inhibits the Formation of the FGF-1 Homodimer in Living Cells. To understand whether AMX attenuates the stress-induced formation of the FGF-1 homodimer in living cells, we evaluated the level of the FGF-1 homodimer in AMX-treated cells at normal and heat-shock conditions. NIH 3T3 cells stably transfected with FGF-1 were subjected to AMX treatment followed by heat shock in the presence of AMX (Figure 6C). About $^1/_{10}$ of the total FGF-1 content is released at heat shock (*7*, *28*). The concentration of AMX used in our experiments (0.375 mM) is known to induce about 80% inhibition of FGF-1 export (*13*), and we observed a similar suppression of FGF-1 export (lower panel of Figure 6C). Because the isolation of FGF-1 from conditioned medium requires the reduction of released dimers to allow the efficient FGF-1 binding to heparin (*7*, *28*), conditioned medium-derived FGF-1 was detected as a monomer. To prevent reduction of the intracellular FGF-1 homodimers, cell lysates were electrophoretically resolved in mercaptoethanol-free conditions. Heat shock induced a significant decrease of the intracellular levels of mono- and dimeric FGF-1 in both AMX-treated and untreated cell lysates (upper and middle panels of Figure 6C), which can be explained by the stress-induced downregulation of protein synthesis. It was observed that AMX treatment resulted in a specific strong reduction of the FGF-1 homodimer but not the FGF-1 monomer level, at both stress and normal conditions (upper and middle panels of Figure 6C). These results indicate that AMX-dependent attenuation of FGF-1 dimerization occurs both in cell-free conditions and in the cell culture.

Results of this study clearly demonstrate that AMX binds to FGF-1 at a site proximal to Cys30 and inhibits the formation of the copper-induced homodimer both in cell-free conditions and in living cells. AMX-mediated inhibition of the release of FGF-1 through the nonclassical pathway appears to be primarily due to the abolition of the formation of the FGF-1 homodimer. In the presence of the drug, FGF-1 is entrapped inside the cell and is unable to be secreted into the extracellular compartment in response to stress conditions. Therefore, it appears that formation of the homodimer is mandatory for the release of FGF-1 into an extracellular compartment under stress. The finding

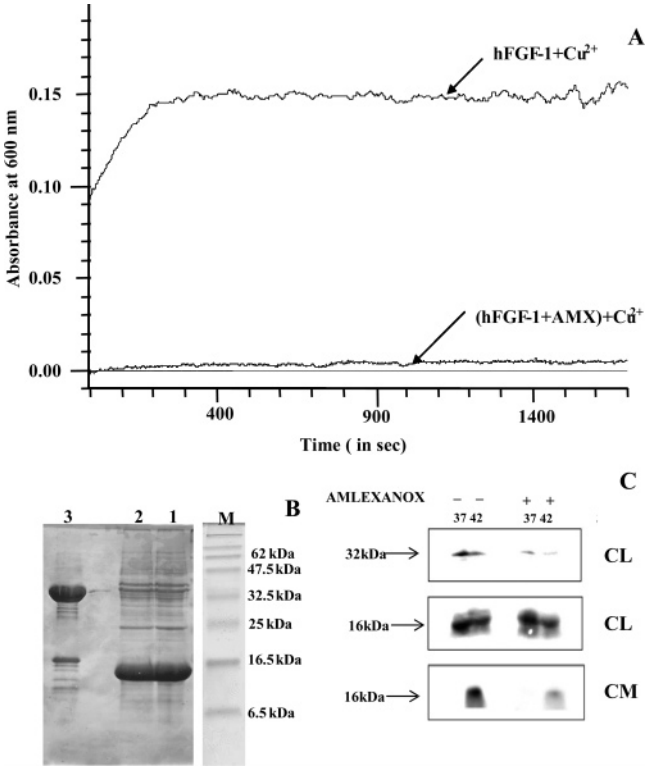

FIGURE 6: (A) Turbidometric assay to monitor the formation of the FGF-1 homodimer. The homodimer of FGF-1 has a tendency to aggregate with time. Therefore, the formation of the homodimer is monitored by the change in absorbance at 600 nm. It could be observed that, in the presence of AMX, the change in absorbance (at 600 nm) is insignificant, suggesting that the drug inhibits the formation of the homodimer. (B) SDS−PAGE analysis of the AMX effect upon the Cu^{2+}-induced FGF-1 dimer formation in a cell-free system, under a nonreducing condition. Lane 1, FGF-1 in the absence of copper; lane 2, FGF-1 in the presence of 50 μM Cu^{2+} and 50 μM AMX; lane 3, FGF-1 in the presence of 50 μM Cu^{2+}. Cu^{2+}-induced homodimer formation is almost completely inhibited in the presence of AMX. (C) Upper panel, FGF-1 homodimer (32 kDa); middle panel, FGF-1 monomer (16 kDa) in cell lysates (CL). The formation of the homodimer is significantly inhibited in the presence of AMX, under both normal and heat-shock conditions, which correlates with the AMX-induced suppression of heat-shock-induced FGF-1 release to the conditioned medium (CM, lower panel).

that AMX specifically inhibits the homodimerization of the potent mitogen FGF-1 provides valuable clues for the rational design of novel pharmacological approaches to the treatment of inflammatory, cardiovascular, and oncological disorders.

ACKNOWLEDGMENT

D. R. and I. G. to partially fulfill the requirements for their Ph.D. degrees performed this work. We express our gratitude to Takeda Chemical Industries for providing amlexanox. We are grateful to the late Dr. Tom Maciag for introducing us to research on the nonclassical export of proteins.

SUPPORTING INFORMATION AVAILABLE

^{1}H-^{15}N chemical-shift perturbation of residues involved in the AMX-binding site and titration curve for Cys30. This material is available free of charge via the Internet at http://pubs.acs.org.

REFERENCES

1. Blobel, G. (2000) Protein targeting (Nobel lecture), *Chembiochem 1*, 86−102.
2. Prudovsky, I., Mandinova, A., Soldi, R., Bagala, C., Graziani, I., Landriscina, M., Tarantini, F., Duarte, M., Bellum, S., Doherty, H., and Maciag, T. (2003) The non-classical export routes: FGF1 and IL-1α point the way, *J. Cell Sci. 116*, 4871−4881.
3. Nickel, W. (2005) Unconventional secretory routes: Direct protein export across the plasma membrane of mammalian cells, *Traffic 8*, 607−614.
4. Burgess, T., and Maciag, T. (1989) The heparin-binding (fibroblast) growth factor family of proteins, *Annu. Rev. Biochem. 58*, 575−606.
5. Arunkumar, A. I., Srisailam, S., Kumar, T. K. S., Kathir, K. M., Chi, Y. H., Wang, H. M., Chang, G. G., Chiu, I., and Yu, C. (2002) Structure and stability of an acidic fibroblast growth factor from *Notophthalmus viridescens*, *J. Biol. Chem. 277*, 46424−46432.
6. Schlessinger, J. (2004) Common and distinct elements in cellular signaling via EGF and FGF receptors, *Science 306*, 1506−1507.
7. Jackson, A., Tarantini, F., Gamble, S., Friedman, S., and Maciag, T. (1995) The release of fibroblast growth factor-1 from NIH 3T3 cells in response to temperature involves the function of cysteine residues, *J. Biol. Chem. 270*, 33−36.
8. Forough, R., Zahn, X., MacPhee, M., Friedman, S., Engleka, K. A., Sayers, T., Wiltrout, R. H., and Maciag, T. (1993) Differential transforming abilities of non-secreted and secreted forms of human fibroblast growth factor-1, *J. Biol. Chem. 268*, 2960−2968.
9. Prudovsky, I., Bagala, C., Tarantini, F., Mandinova, A., Soldi, R., Bellum, S., and Maciag, T. (2002) The intracellular translocation of the components of the fibroblast growth factor 1 release complex precedes their assembly prior to export, *J. Cell. Biol. 158*, 201−208.
10. Tarantini, F., Gamble, S., Jackson A., and Maciag, T. (1995) The cysteine residue responsible for the release of fibroblast growth factor-1 residues in a domain independent of the domain for phosphatidylserine binding, *J. Biol. Chem. 270*, 29039−29042.
11. Engleka, K. A., and Maciag, T. (1992) Inactivation of human fibroblast growth factor-1 (FGF-1) activity by interaction with copper ions involves FGF-1 dimer formation induced by copper-catalyzed oxidation, *J. Biol. Chem. 267*, 11307−11315.
12. Landriscina, M., Bagala, C., Mandinova, A., Soldi, R., Micucci, I., Bellum, S., Prudovsky, I., and Maciag, T. (2001) Copper induces the assembly of a multiprotein aggregate implicated in the release of fibroblast growth factor 1 in response to stress, *J. Biol. Chem. 276*, 25549−25557.
13. Mouta-Carreira, C., LaVallee, T. M., Tarantini, F., Jackson, A., Lathrope, J. T., Hampton, B., Burgess, W. H., and Maciag, T. (1998) S100A13 is involved in the regulation of fibroblast growth factor-1 and p40 synaptotagmin-1 release *in vitro*, *J. Biol. Chem. 273*, 22224−22231.
14. Landriscina, M., Prudovsky, I., Carreira, C. M., Soldi, R., Tarantini, F., and Maciag, T. (2000) Amlexanox reversibly inhibits cell migration and proliferation and induces the Src-dependent disassembly of actin stress fibers *in vitro*, *J. Biol. Chem. 275*, 32753−32762.
15. Madinov, L., Mandinova, A., Kyurkchiev, S., Kehayov, I., Soldi, R., Bagal, C., de Munick, E. D., Linder, V., Post, M. J., Simons, M., Bellum, S., Prudovsky, I., and Maciag, T. (2003) Copper chelation represses the vascular response to injury, *Proc. Natl. Acad. Sci. U.S.A. 100*, 6700−6705.
16. Arunkumar, A. I., Kumar, T. K., Kathir, K. M., Srisailam, S., Wang, H. M., Leena, P. S., Chi, Y. H., Chen, H. C., Wu, C. H., Wu, R. T., Chang, G. G., Chiu, I. M., and Yu, C. (2002) Oligomerization of acidic fibroblast growth factor is not a prerequisite for its cell proliferation activity, *Protein Sci. 11*, 1050−1061.
17. Ogura, K., Nagata, K., Hatanaka, H., Habuchi, H., Kimata, K., Tati, S., Raveru, M. W., Jaye, M., Schlessinger, J., and Inagaki, F. (1999) Solution structure of human acidic fibroblast growth factor and interaction with heparin-derived hexasaccharide, *J. Biomol. NMR 13*, 11−24.
18. Goddard, T. D., and Kneller, D. G. *SPARKY 3*, University of California, San Francisco, CA.
19. Palma, P. N., Krippahl, L., Wampler, J. E., and Moura, J. J. (2000) BiGGER: A new (soft) docking algorithm for predicting protein interactions, *Proteins 39*, 372−384.

20. Koradi, R., Billeter, and Wurthrich K. (1996) MOLMOL: A program for display and analysis of macromolecular structures, *J. Mol. Graphics 14*, 29−32, 51−55.
21. Chi, Y. H., Kumar, T. K. S., Kathir, K. M., Lin, D. H., Zhu, X., Chiu, I. M., and Yu, C. (2002) Investigation of the structural stability of the human acidic fibroblast growth factor by hydrogen−deuterium exchange, *Biochemistry 85*, 459−472.
22. Srimathi, T., Kumar, T. K. S., Chi, Y. H., Chiu, I. M., and Yu, C. (2002) Characterization of the structure and dynamics of a near-native equilibrium intermediate in the unfolding pathway of an all β-barrel protein, *J. Biol. Chem. 277*, 47507−47516.
23. Ridinger, K., Schafer, B. W., Durussel, I., Cox, J. A., and Heizmann, C. W. (2000) S100A13. Biochemical characterization and subcellular localization in different cell lines, *J. Biol. Chem. 275*, 8686−8694.
24. Nakamura, S., and Kidokoro, S. (2004) Direct observation of the enthalpy change accompanying the native to molten-globule transition of cytochrome *c* by using isothermal acid-titration calorimetry, *Biophys. Chem. 109*, 229−249.
25. Wang, L., and Kallenbach, N. R. (1998) Proteolysis as a measure of the free energy difference between cytochrome *c* and its derivatives, *Protein Sci. 7*, 2360−2464.
26. Hajduk, P. J., Meadows, R. P., and Fesik, S. W. (1999) NMR-based screening in drug discovery, *Q. Rev. Biophys. 32*, 211−240.
27. Krishna, M. M., Hoang, L., Lin, Y., and Englander, S. W. (2004) Hydrogen exchange methods to study protein folding, *Methods 43*, 51−64.
28. Jackson, A., Friedman, S., Zhan, X., Engleka K. A., Forough, R., and Maciag, T. (1992) Heat shock induces the release of fibroblast growth factor 1 from NIH 3T3 cells, *Proc. Natl. Acad. Sci. U.S.A. 89*, 10691−10695.

BI0516071